Journal of the American College of Cardiology Vol. 58, No. 11, 2011

Published by Elsevier Inc.
ISSN 0735-1097/$36.00
doi:10.1016/j.jacc.2011.03.063

Strain-Encoded Cardiac Magnetic Resonance During High-Dose Dobutamine Stress Testing for the Estimation of Cardiac Outcomes

Comparison to Clinical Parameters and Conventional Wall Motion Readings

Grigorios Korosoglou, MD,* Gitsios Gitsioudis, MD,* Andreas Voss, PHD,† Stephanie Lehrke, MD,* Nina Riedle, MD,* Sebastian J. Buss, MD,* Christian Zugck, MD,* Evangelos Giannitsis, MD,* Nael F. Osman, PHD,‡§ Hugo A. Katus, MD*

Heidelberg, Germany; Baltimore, Maryland; and Cairo, Egypt

Objectives The purpose of this study was to determine the prognostic value of strain-encoded magnetic resonance imaging (SENC) during high-dose dobutamine stress cardiac magnetic resonance imaging (DS-MRI) compared with conventional wall motion readings.

Background Detection of inducible ischemia by DS-MRI on the basis of assessing cine images is subjective and depends on the experience of the readers, which may influence not only the diagnostic classification but also the risk stratification of patients with ischemic heart disease.

Methods In all, 320 consecutive patients with suspected or known coronary artery disease underwent DS-MRI, using a standard protocol in a 1.5T MR scanner. Wall motion abnormalities (WMA) and myocardial strain were assessed at baseline and during stress, and outcome data including cardiac deaths, nonfatal myocardial infarctions ("hard events"), and revascularization procedures performed >90 days after the MR scans were collected.

Results Thirty-five hard events occurred during a 28 ± 9 month follow-up period, including 10 cardiac deaths and 25 nonfatal myocardial infarctions, and 32 patients underwent coronary revascularization. Using a series of Cox proportional-hazards models, both resting and inducible WMA offered incremental information for the assessment of hard cardiac events compared to clinical variables (chi-square = 13.0 for clinical vs. chi-square = 26.1 by adding resting WMA, $p < 0.001$, vs. chi-square = 39.3 by adding inducible WMA, $p < 0.001$). Adding visual SENC or quantitative strain rate reserve to this model further improved the prediction of outcome (chi-square = 50.7 vs. chi-square = 52.5, $p < 0.001$ for both). In a subset of patients (n = 175) who underwent coronary angiography, SENC yielded significantly higher sensitivity for coronary artery disease detection (96% vs. 84%, $p < 0.02$), whereas specificity and accuracy were not significantly different (88% vs. 94% and 93% vs. 88%, p = NS for both).

Conclusions Strain-encoded MRI aids the accurate identification of patients at high risk for future cardiac events and revascularization procedures, beyond the assessment of conventional atherogenic risk factors and resting or inducible WMA on cine images. (Strain-Encoded Cardiac Magnetic Resonance Imaging as an Adjunct for Dobutamine Stress Testing; NCT00758654) (J Am Coll Cardiol 2011;58:1140–9) © 2011 by the American College of Cardiology Foundation

High-dose dobutamine stress (DS) cardiac magnetic resonance imaging (MRI) is a well-established diagnostic modality for the noninvasive detection of inducible myocardial ischemia (1,2) and for the risk stratification of patients with

See page 1150

From the *Department of Cardiology, University of Heidelberg, Heidelberg, Germany; †Institute of Psychology, University of Heidelberg, Heidelberg, Germany; ‡Russell H. Morgan Department of Radiology and Radiological Science, The Johns Hopkins University School of Medicine, Baltimore, Maryland; and the §Nile University, Cairo, Egypt. Dr. Osman is a founder and shareholder in Diagnosoft, Inc., the software used for the analysis of the acquired SENC images. All other authors have reported that they have no relationships relevant to the contents of this paper to disclose.

Manuscript received October 20, 2010; revised manuscript received February 28, 2011, accepted March 22, 2011.

coronary artery disease (CAD) (3,4). However, currently the detection of inducible ischemia by DS-MRI is based on the assessment of cine images, which is subjective and depends on the experience of the readers. That may influence not only the diagnostic classification but also the risk stratification of patients with ischemic heart disease.

The ability of strain-encoded magnetic resonance imaging (SENC) to detect CAD with higher sensitivity and in earlier stages of inotropic stimulation than conventional cine imaging was recently demonstrated (5,6). In this regard, it is conceivable that strain abnormalities during stress, which are detectable by SENC and missed by conventional wall motion readings, may significantly impact clinical outcome in patients with suspected or known CAD. Therefore, in the present study, we sought to determine the potential of SENC to predict future cardiac events in patients who underwent DS-MRI. The results were compared to clinical parameters and to conventional wall motion readings on cine images. Furthermore, analysis of subgroups was conducted to evaluate the usefulness of SENC in patients with low, intermediate, and high pre-test probability using the Duke Clinical Score.

Abbreviations and Acronyms

CAD = coronary artery disease
DS = dobutamine stress
MR = magnetic resonance
MRI = magnetic resonance imaging
RWMA = resting wall motion abnormality
SENC = strain-encoded magnetic resonance imaging
WMA = wall motion abnormality

Methods

Patient population. From January 2006 to December 2009, patients with suspected or known CAD underwent clinically indicated DS-MRI. Subjects were excluded because of non–sinus rhythm, unstable angina, severe arterial hypertension (>200/120 mm Hg), moderate or severe valvular disease, and general contraindications to MR examination. All procedures complied with the Declaration of Helsinki and were approved by our local ethics committee, and all patients gave written informed consent.

In all, 382 patients were screened, and diagnostic stress examinations were obtained in 324 patients. Reasons for discontinuation of the imaging procedure included claustrophobia (n = 8), large body habitus (n = 13), arrhythmias during stress (n = 17), limiting side effects (n = 5), and failure to achieve the target heart rate (n = 15). Furthermore, during the follow-up, 4 patients (1%) were lost, so that 320 patients had complete stress MRI and follow-up information, and constituted our patient population.

Traditional risk factors for CAD, including arterial hypertension, hyperlipidemia, current or prior smoking, diabetes mellitus, and family history of CAD were recorded at the time of imaging. Furthermore, the total number of atherogenic risk factors (range 0 to 5) and the Duke Clinical Score, which incorporates type of chest discomfort, age, sex, and traditional atherogenic risk factors (7) were calculated. Hereby, patients were categorized into a low (<30%), intermediate (30% to 70%), or high (>70%) pre-test probability group for CAD (4,8).

Cardiovascular MR examination. Subjects were examined in a clinical 1.5-T whole-body MR scanner Achieva system (Philips Medical Systems, Best, the Netherlands). Stress cardiovascular MR images were acquired at rest and during a standardized high-dose dobutamine/atropine protocol during a total study duration of ~35 to 40 min (Online Fig. 1) (4). Four-, 2-, and 3-chamber views and 3 short-axis views (apical, mid-ventricular, and basal) were used. Electrocardiographic rhythm and symptoms were monitored continuously, and blood pressure was measured every 3 min. Dobutamine was infused intravenously during 3-min stages, at incremental doses of 10, 20, 30, and 40 μg/kg of body weight per minute until ≥85% of the age-predicted heart rate was reached (220 − age). If at the peak dose of dobutamine infusion the target heart rate was not achieved, atropine was administered in 0.25-mg increments to a maximal dose of 2.0 mg. Stress testing was discontinued when the target heart rate was achieved, or when 1 of the following occurred: new WMA in ≥2 adjacent segments, severe chest pain or dyspnea, decrease in systolic blood pressure of ≥40 mm Hg, severe arterial hypertension of ≥220/120 mm Hg, or severe arrhythmias. In the absence of ischemia, failure to attain 85% of age-predicted maximal heart rate was considered as a nondiagnostic result.

CINE IMAGING. A steady-state free precession sequence was used to obtain the cine images of the 4-, 2-, and 3-chamber view and 3 short-axis planes (apical, mid-ventricular and basal) with an 8-mm slice thickness. Typical parameters were as follows: field of view = 350 × 350 mm^2, matrix size = 160 × 160, flip angle = 60°, repetition time (TR) = 2.8 ms; echo time (TE) = 1.4 ms, and acquired voxel size = 2.2 × 2.2 × 8 mm^3. The temporal resolution was 21 ms to 28 ms, and the total scan duration was 7 to 12 s. Cine images were acquired at baseline, and acquisitions were repeated during each stage including the peak level of dobutamine administration.

STRAIN-ENCODED MRI. With the SENC pulse sequence, radiofrequency pulses with ramped flip angles are applied to compensate for the tag fading caused by longitudinal relaxation and to maintain constant myocardial signal intensity throughout the cardiac cycle (9). By combining SENC magnitude images at 2 different tuning frequencies (low and high tuning), a SENC strain map is computed, which is then overlaid pixel by pixel on the anatomical image. In this way, color-coded SENC functional images (maximum contraction illustrated as red, and lack of contraction illustrated as white) are generated. The SENC images were acquired at the same plane levels as that used for cine scans with 10-mm slice thickness. Typical parameters were as follows: field of view = 350 × 350 mm^2, matrix size = 80 × 80, flip angle = 30°, TR = 25 ms, TE = 0.9 ms, and acquired voxel size = 4.4 ×

JACC Vol. 58, No. 11, 2011
September 6, 2011:1140–9

4.4×10 mm^3. Strain-encoded images were acquired at baseline and during peak dobutamine administration. The temporal resolution (range 15 to 25 ms) and the number of acquired cardiac phases (typically between 24 and 48) were individually adjusted according to the achieved heart rate during baseline and each inotropic stage, to cover >90% of the cardiac cycle.

Visual interpretation of cine and SENC images. For interpretation of wall motion, corresponding rest and stress cine images were displayed using View Forum software (Philips Medical Systems, Best, the Netherlands). Segmental wall motion was graded semiquantitatively using a 16-segment model according to American Heart Association guidelines (10), and a 3-point scale (0 = normal wall motion, 1 = hypokinesia, 2 = akinesia or dyskinesia); and inducible ischemia was considered present in cases of new or worsening WMA of ≥1 grade during stress. In addition, in segments with resting wall motion abnormalities intermediate stress phases were systematically analyzed. Thereby, segments with resting wall motion abnormalities that: 1) showed direct worsening with no improvement at any stages; or 2) improved during intermediate stress and subsequently deteriorated during peak stress ("biphasic response") were classified as ischemic (11).

Corresponding baseline and peak stress SENC images were displayed using Diagnosoft SENC, version 1.06 (Diagnosoft, Inc., Palo Alto, California), a software package that allows the color-encoded interpretation of myocardial strain on SENC images. Myocardial strain was graded semiquantitatively using a 3-point color scale (5,6): 0 = normal strain corresponding to red myocardium, 1 = reduced strain corresponding to faded orange/yellowish myocardium, 2 = severely reduced or absent strain corresponding to white myocardium. For visual interpretation, differences in the color scale were carefully evaluated at baseline and during peak stress in corresponding myocardial segments, and inducible ischemia was considered present in case of strain reduction of ≥1 grade. Cine and SENC images were evaluated visually by 2 independent observers who were both blinded to clinical data.

Quantitative analysis of SENC images. For quantification analysis, the temporal course of regional myocardial strain was registered throughout the cardiac cycle in each segment, and quadratic interpolation was used to estimate the time derivative of the systolic strain and to calculate the peak systolic strain (S expressed in %) and the peak systolic strain rate (SR expressed in 1/s). The ratios

$$S_{Reserve} = \frac{S_{peak\text{-}stress}}{S_{baseline}} \text{ and } SR_{Reserve} = \frac{SR_{peak\text{-}stress}}{SR_{baseline}}$$

were generated to evaluate strain and strain rate response, respectively, during DS-MRI. For analysis by patients, in patients without inducible ischemia, mean strain and strain rate reserve were calculated in all segments, whereas in patients with inducible strain defects on SENC images, the mean strain and strain rate reserve were calculated in the ischemic region.

Follow-up data and definition of study endpoints. Personnel unaware of the stress results contacted each subject or an immediate family member, and the date of this contact was used for the calculation of the follow-up time duration. Outcome data were collected from a standardized questionnaire and determined from patient interviews at the outpatient clinic or by telephone interviews. Reported clinical events were confirmed by review of the corresponding medical records in our electronic Hospital Information System, and contact with the general practitioner, referring cardiologist, or the treating hospital. Cardiac death and nonfatal myocardial infarction were registered as "hard events." Other events included clinically indicated revascularization by percutaneous coronary intervention or coronary artery bypass graft surgery. Because the results of the MR examination may have triggered revascularization procedures, thereby altering the subsequent event rate, "early" revascularization within 3 months of MRI was not considered, and patients were censored at the time of the revascularization procedures.

Coronary angiography. In a subset of 175 patients, invasive coronary angiography was obtained for clinical reasons within 3 weeks from the DS-MRI study and deemed as the anatomical standard reference for the detection of CAD. The procedure was performed according to the angiographic guidelines, and at least 2 orthogonal views of every major coronary vessel and its side branches were acquired. Diameter stenoses ≥50% were considered as inductive of ischemia during inotropic stimulation.

Statistical analysis. Analysis was performed using commercially available software (MedCalc 9.3, Mariakerke, Belgium). Continuous variables were expressed as mean ± SD, and categorical variables as proportions. Repeated-measures analysis of variance with Bonferroni correction for multiple comparisons was used to compare continuous variables. Group differences between ordinal variables were tested using the exact Mann-Whitney test, and differences between nominal variables were assessed using Fisher exact tests. All tests were 2-tailed. Agreement between the 2 observers interpreting cine and SENC images was assessed using kappa statistics (12). Intraobserver and interobserver variability for quantification of myocardial strain were calculated by repeated analysis of representative regions of interest for strain and strain rate in 40 randomly selected SENC images. The time spent for the post-processing of the acquired SENC data was also documented. The readings were separated by 8 weeks to minimize recall bias. Based on the results of coronary angiography (i.e., <50% or ≥50% stenosis) receiver-operating characteristics (ROC) were used to determine the diagnostic value WMA, SENC, $S_{Reserve}$, and $SR_{Reserve}$ for the detection of inducible ischemia. Hereby, cut-off values were determined for $S_{Reserve}$ and $SR_{Reserve}$ to provide an optimal trade-off between sensitivity and specificity. For survival analysis, Kaplan-Meier curves were used to estimate the distribution of

Table 1 Detection of Coronary Artery Disease by Cine, Visual, and Quantitative SENC

	Sensitivity	Specificity	PPV	NPV	Accuracy	AUC
Cine imaging	84% (76%–91%)	94% (85%–98%)	96%	79%	88%	0.89
Visual SENC	96%* (91%–99%)	88% (78%–95%)	93%	94%	93%	0.92
Strain reserve, cutoff = 0.94	71% (61%–79%)	92% (83%–98%)	94%	66%	78%	0.88
Strain rate reserve, cutoff = 1.75	95% (88%–98%)	92% (83%–97%)	95%	91%	93%	0.96

Values are percent of patients (95% confidence interval) or percent of patients. *$p < 0.05$ for visual strain-encoded magnetic resonance imaging (SENC) versus cine imaging (by exact 2-sided McNemar tests).
AUC = area under the curve; NPV = negative predictive value; PPV = positive predictive value.

cardiac events as a function of the follow-up duration, and the association of cine and SENC findings with outcomes was investigated using Cox proportional-hazards models and univariate and multivariable procedures. Furthermore, a series of Cox proportional-hazards models was assessed including the following hierarchical steps: 1) total number of atherogenic risk factors (referred to as clinical data); 2) resting WMA; 3) inducible WMA by cine imaging; and 4) visual SENC or strain reserve or strain rate reserve indices. Model chi-square was then compared for each incremental step. In addition, integrated discrimination improvement analysis was performed using the same hier-

Table 2 Demographic and Baseline MRI Data of Patients With and Without Hard Cardiac Events

Parameters	All Patients (n = 320)	Patients Without Hard Events (n = 285)	Patients With Hard Events (n = 35)	p Value
Clinical data				
Age, yrs	64 ± 14	63 ± 15	69 ± 8	<0.001
Male	236 (74%)	207 (73%)	29 (83%)	0.32
Body mass index, kg/m^2	26 ± 4	26 ± 4	25 ± 4	0.08
Typical angina	81 (25%)	73 (26%)	8 (23%)	0.72
Arterial hypertension	242 (76%)	212 (74%)	30 (86%)	0.32
Hyperlipidemia	180 (56%)	153 (54%)	27 (77%)	0.03
Diabetes mellitus	69 (22%)	55 (19%)	14 (40%)	0.05
Smoking	71 (22%)	57 (20%)	14 (40%)	0.06
Family history of CAD	75 (23%)	66 (23%)	9 (26%)	0.82
Known CAD	145 (45%)	126 (44%)	19 (54%)	0.27
Total risk factors, range 0 to 5	2.0 ± 1.2	1.9 ± 1.2	2.7 ± 0.9	<0.001
Prior PCI	79 (25%)	66 (23%)	13 (37%)	0.11
Prior CABG	17 (5%)	15 (5%)	2 (6%)	0.91
Prior myocardial infarction	61 (19%)	49 (17%)	12 (34%)	0.015
Pre-test probability by Duke clinical score, %	54 ± 35	51 ± 35	72 ± 27	<0.001
Cardiac medications				
Aspirin, 100 mg/day	170 (53%)	144 (51%)	26 (74%)	0.005
Clopidogrel, 75 mg/day	31 (10%)	28 (10%)	3 (9%)	0.81
Beta-blockers	233 (73%)	207 (73%)	26 (74%)	0.83
ACE inhibitors	172 (54%)	154 (54%)	18 (51%)	0.84
Angiotensin-receptor blockers	74 (23%)	69 (24%)	5 (14%)	0.13
Statins	183 (57%)	160 (56%)	23 (66%)	0.28
Calcium-channel blockers	63 (20%)	55 (19%)	8 (23%)	0.64
Diuretics	79 (25%)	67 (24%)	12 (34%)	0.21
Baseline MRI data				
LVEF, %	57 ± 18	57 ± 18	50 ± 11	0.001
EDV, ml	161 ± 47	158 ± 47	189 ± 38	<0.001
ESV, ml	73 ± 45	70 ± 45	97 ± 34	<0.001
Resting wall motion abnormalities	90 (28%)	70 (25%)	20 (57%)	<0.001
Baseline hemodynamics				
Mean blood pressure, mm Hg	88 ± 14	88 ± 14	85 ± 14	0.25
Heart rate, beats/min	67 ± 15	67 ± 15	66 ± 11	0.47
Stress hemodynamics				
Mean blood pressure, mm Hg	109 ± 24	111 ± 23	99 ± 18	0.001
Heart rate, beats/min	138 ± 14	139 ± 13	127 ± 14	<0.001

Values are mean ± SD or n (%).
ACE = angiotensin-converting enzyme; BMI = body mass index; CABG = coronary artery bypass graft surgery; CAD = coronary artery disease; EDV = end-diastolic volume; ESV = end-systolic volume; LVEF = left ventricular ejection fraction; MRI = magnetic resonance imaging; PCI = percutaneous coronary intervention.

archical model (13). Differences in diagnostic value between cine and SENC for CAD detection (stenosis ≥50%) were evaluated using exact 2-sided McNemar chi-square tests. Differences were considered statistically significant at $p < 0.05$.

Results

Safety and feasibility issues. No myocardial infarctions and fatal complications occurred during imaging. Severe side effects requiring the termination of the study occurred in 3 (0.9%) patients due to sustained ventricular tachycardia (n = 2) and severe hypotension (n = 1). Of 10,240 segments available for analysis at baseline and during stress, evaluation of segmental wall motion not was feasible in 52 segments (0.5%). Visual evaluation of myocardial strain with SENC images not was feasible in 124 segments (1.2%), and quantification of myocardial strain and strain rate despite visually acceptable image quality was not deemed appropriate in a further 142 segments (2.6%). Resting wall motion abnormalities (RWMA) were observed in 90 of 320 patients (28%), and 19 of 90 patients (21%) exhibiting RWMA showed a biphasic response during stress.

Results of coronary angiography. Coronary angiography showed ≥50% stenosis in 109 of 175 patients (62%), including 54 with single-vessel disease and 55 with multivessel disease. SENC yielded significantly higher sensitivity for CAD detection (96% vs. 84%, $p < 0.02$), while specificity and accuracy were similar (88% vs. 94% and 93% vs. 88%, p = not significant for both). Furthermore, strain, and especially strain rate reserve, provided high accuracy for CAD detection (Online Fig. 2). Diagnostic values are summarized in Table 1.

Outcomes. During the follow-up period (28 ± 9 months), 35 hard events occurred, including 10 cardiac deaths and 25 nonfatal infarctions. In 41 patients, early revascularization was performed (30 ± 25 days), and 32 patients underwent late revascularization (27 by PCI and 5 by CABG). The baseline characteristics, hemodynamic data, and MR parameters of patients with hard events (n = 35) and without hard events (n = 285) are illustrated in Table 2.

Survival analysis. Kaplan-Meier curves based on stress MR findings including conventional wall motion analysis and SENC are shown in Figure 1. The presence of both inducible WMA and strain defects was associated with a

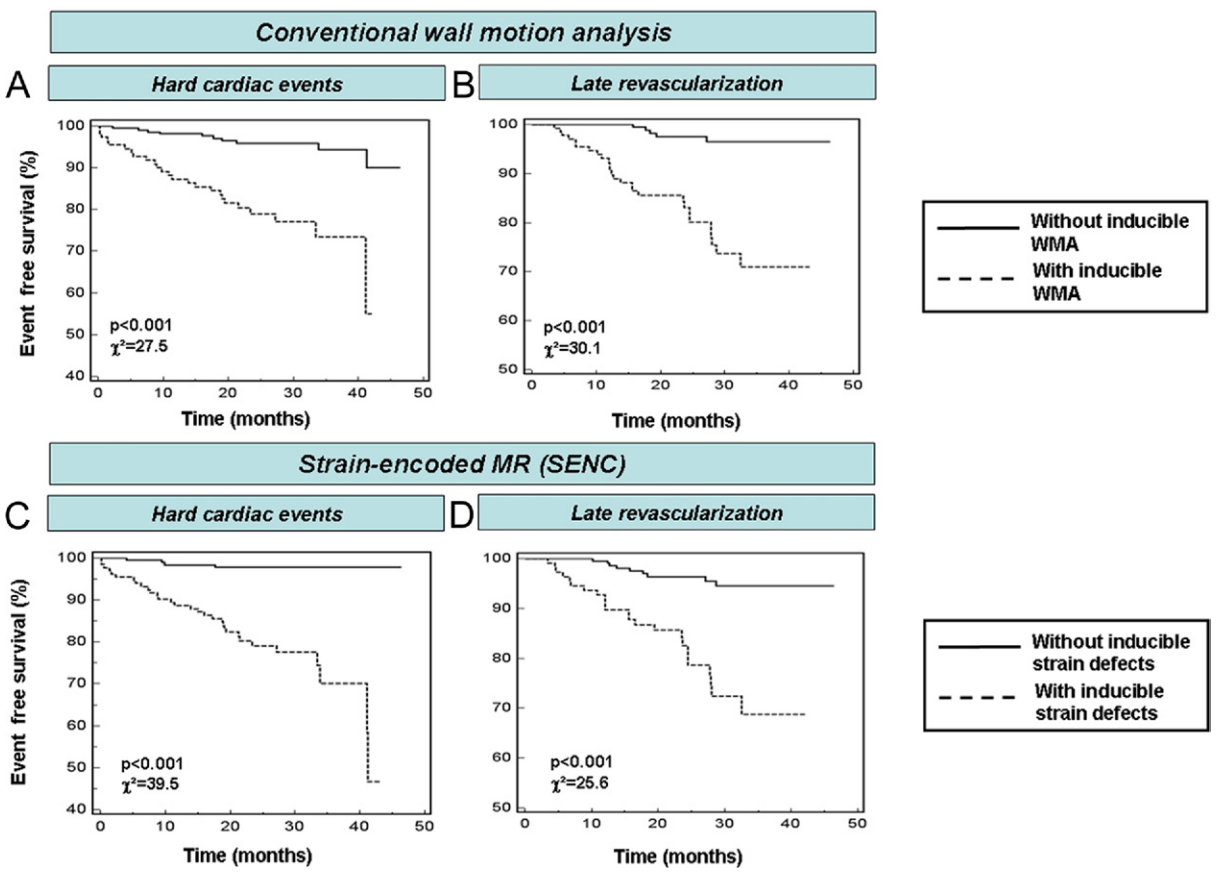

Figure 1 Survival Analysis on Basis of WMA and SENC

The presence of both inducible wall motion abnormality (WMA) and strain defects **(dashed lines)** was associated with a higher rate of **(A, C)** hard events and **(B, D)** revascularization procedures, compared to patients with normal wall motion and strain response **(solid lines)** during stress testing. MR = magnetic resonance; SENC = strain-encoded magnetic resonance imaging.

higher rate of hard events (Figs. 1A and 1C) and revascularization procedures (Figs. 1B and 1D).

Furthermore, a significant higher rate for hard cardiac events was observed among patients with RWMA versus without RWMA. In patients with RWMA, a biphasic response during stress testing was indicative of worse outcome; whereas inducible WMA was predictive of hard cardiac events both in patients with and without RWMA (Online Fig. 3).

Univariate and multivariate analysis. By univariate analysis, significant associations were observed among several clinical parameters and baseline and stress MRI findings by cine and SENC for both hard events and revascularization procedures (Fig. 2).

Using multivariate analysis, resting and inducible WMA on cine imaging and the total number of atherogenic risk factors were independently associated with hard events and late revascularization. When inducible strain defects were additionally considered in the model, however, inducible WMA was no longer predictive, and SENC yielded the strongest independent association with outcome (Fig. 3).

Incremental value of visual and quantitative SENC over cine imaging. Using a series of Cox models, resting and inducible WMA both offered incremental information for the assessment of hard cardiac events compared to clinical data. Adding visual SENC or quantification of myocardial strain rate reserve to the model further improved prediction of outcome (Fig. 4A). The incremental value of visual SENC and strain rate reserve beyond the assessment of clinical variables, and WMA was confirmed using integrated discrimination improvement analysis (Online Fig. 4).

Subgroup analysis. Dividing patients by pre-test probability showed that the incremental value of SENC mainly derived from significantly better risk stratification of patients with intermediate pre-test probability (Fig. 4B). This finding was confirmed by Kaplan-Meier analysis, in which patients with intermediate pre-test probability and normal strain response exhibited no hard events, whereas patients with normal wall motion response still experienced a cumulative event rate of >5% (Figs. 5C and 5D). Conversely the discriminative potential of the 2 techniques was similar in the other subgroups (Figs. 5A, 5B, 5E, and 5F).

Observer agreement and variabilities and time spent. Agreement between observers interpreting cine and SENC images was 88% (k = 0.78) and 86% (k = 0.76), respectively. SENC allowed for reproducible quantification of strain and strain rate, showing intraobserver and interobserver variabilities of 6.6% and 9.5% for strain and 7.7% and 10.1% for strain rate, respectively. Quantification of myocardial strain and strain rate resulted in an additional time spent of 18.5 ± 5.4 min per patient.

Discussion

Our study demonstrates the ability of an MRI-based strain imaging technique (SENC) to assess future hard cardiac events and revascularization procedures beyond clinical

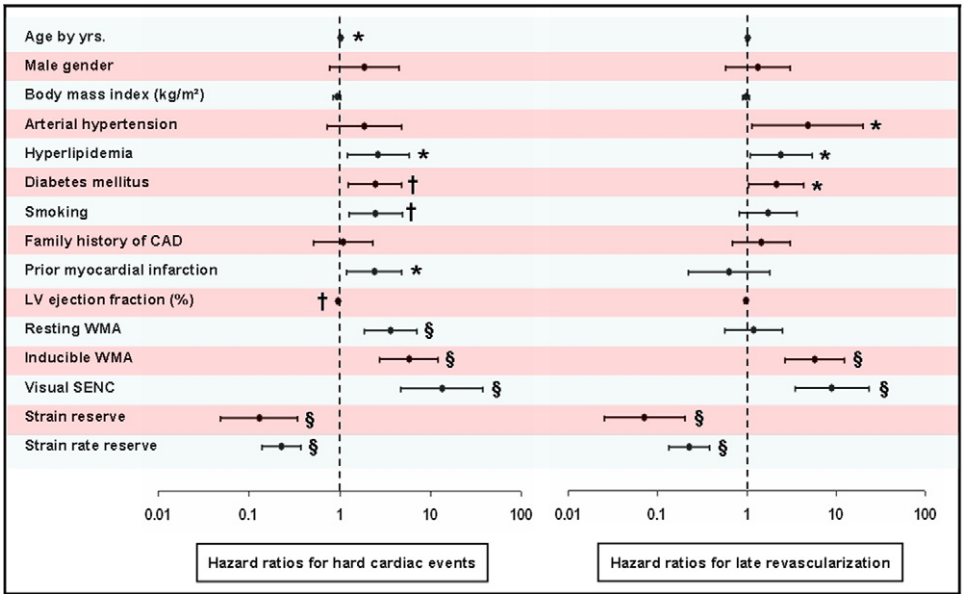

Figure 2 Univariate Value of Clinical Parameters, Baseline, and Stress Magnetic Resonance

Significant associations were observed between several clinical parameters, baseline ejection fraction, and resting and inducible WMA, and by visual and quantitative SENC with future hard events and revascularization procedures. *p < 0.05; †p < 0.01; §p < 0.001. CAD = coronary artery disease; LV = left ventricular; other abbreviations as in Figure 1.

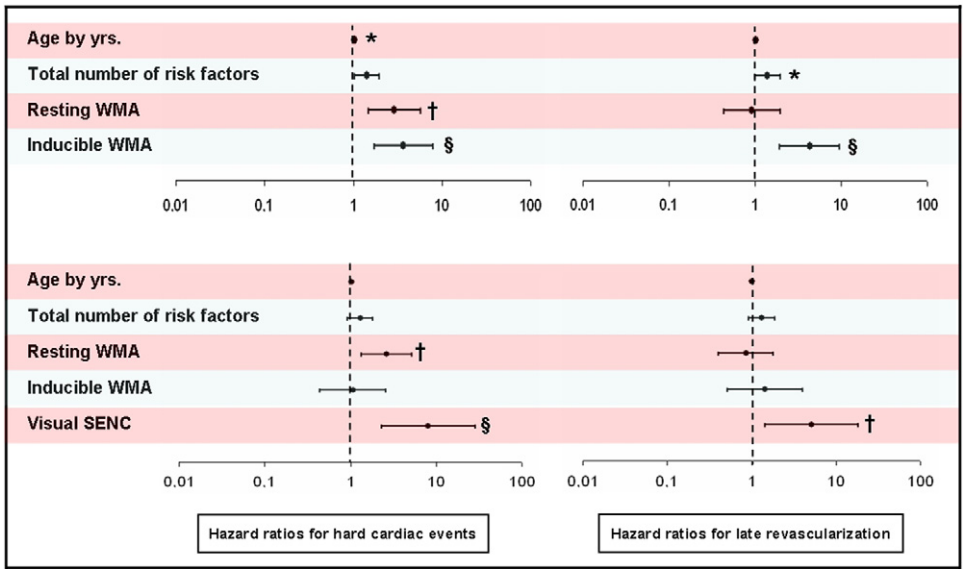

Figure 3 **Multivariate Value of Clinical Parameters, Baseline, and Stress Magnetic Resonance**

Using multivariable analysis, resting and inducible WMA detected by cine imaging and the total number of atherogenic risk factors was independently associated with hard cardiac events. When inducible strain defects were additionally considered in the model, however, inducible WMA were no longer predictive, and SENC yielded the strongest independent association with outcome. Similar associations were observed for the prediction of revascularization procedures. *$p < 0.05$; †$p < 0.01$; §$p < 0.001$. Abbreviations as in Figure 1.

parameters, baseline ejection fraction, and the assessment of inducible WMA during dobutamine stress testing.

Previous studies demonstrated the ability of echocardiographic strain imaging techniques (tissue Doppler, speckle tracking) to predict outcome (14,15). However, echocardiography is generally associated with problems that are inherent in the use of Doppler, and are related to signal noise and angle dependency (16), so that tomographic imaging modalities like MRI would be preferable. Recently, we demonstrated that the direct color-coded visualization of myocardial strain with SENC provides objective detection of differences in regional myocardial strain, yielding significantly higher sensitivity than conventional wall motion readings for the detection of CAD (5,6). That is now confirmed in our entire patient population. Furthermore, we demonstrated that both visual SENC and quantitative assessment of myocardial strain rate are predictive of clinical outcome, including hard cardiac events and subsequent revascularization procedures. In this regard, the visual evaluation of strain on SENC images without the need for quantification assessment offered incremental prognostic information beyond the assessment of clinical variables and resting or inducible WMA on cine images. That may be attributed to the higher sensitivity of circumferential and longitudinal strain to detect dynamic changes in myocardial function (17–20), compared to cine images, which primarily track radial function of the myocardium. Thus, the implementation of color maps provided by SENC in the clinical routine may further aid not only the diagnostic classification but also the risk stratification of patients with ischemic heart disease.

It should be noted that the presence of resting WMA had significant impact on clinical outcome, as it proved significant both in the univariate and in the multivariate analysis after the consideration of clinical parameters and inducible ischemia. Furthermore, quantitative estimation of strain rate but not strain reserve offered incremental value to conventional WMA for the assessment of clinical outcome. This finding seems to be in agreement with the higher sensitivity of strain rate compared to strain reserve for the detection of ischemic myocardium during inotropic stimulation, while the value of strain reserve was lower to that provided by visual analysis (5,6). Along the same line, previous echocardiographic studies demonstrated the superiority of strain rate compared to systolic strain for the detection of functionally significant CAD in humans (21). Similarly, experimental data showed that strain rate better reflects changes in regional myocardial contractile behavior, in contrast to alterations in systolic strain, which can also be related to increased heart rate or to altered loading conditions (22). However, even quantitative estimation of the myocardial strain rate did not add incremental prognostic information beyond the assessment of visual SENC. On the basis of that and in light of the time spent and the need of sophisticated post-possessing software for quantification of the acquired data, the applicability of strain quantification approaches in the clinical routine is questionable. Thus, the color-coded visualization of myocardial strain may be preferable in daily routine practice, especially with less trained observers, where color differences might be easier to interpret than the assessment of myocardial motion on cine images.

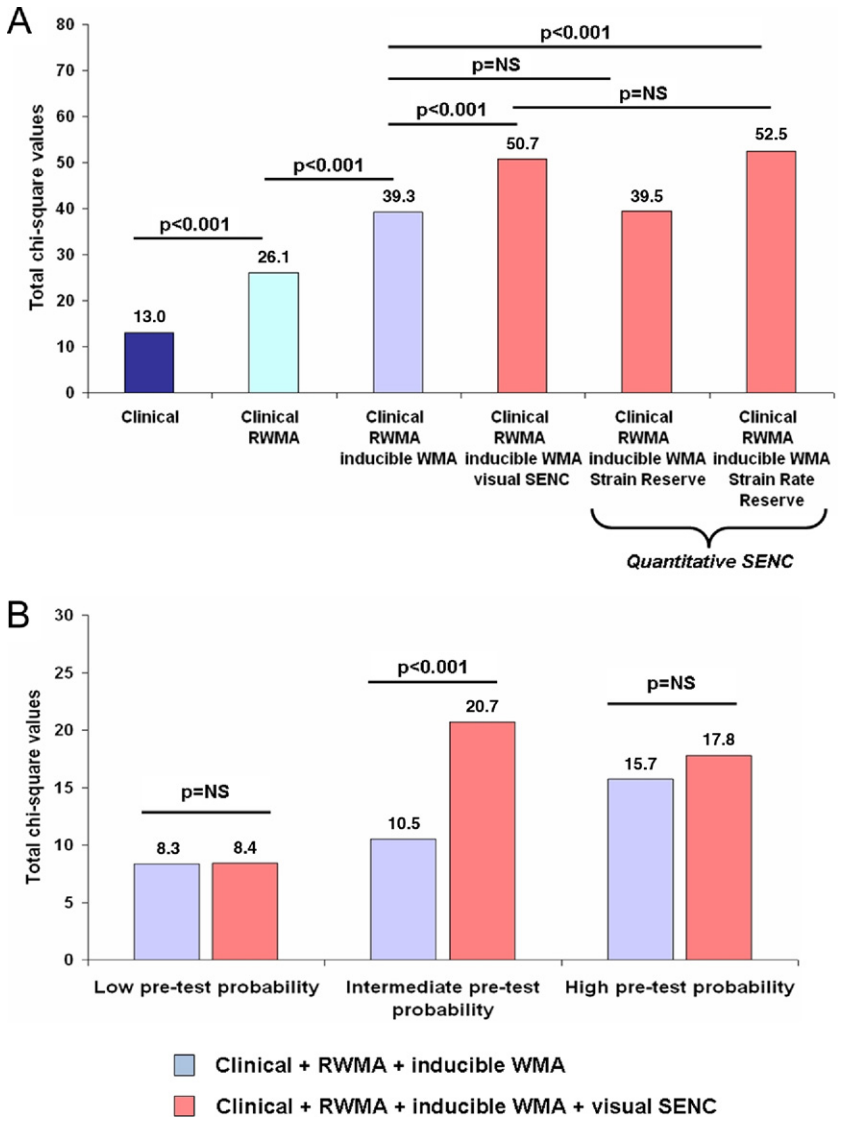

Figure 4 **Incremental Value of Visual and Strain Rate Reserve Quantification Beyond Inducible WMA by Cine Imaging**

In a series of Cox models evaluated for the prediction of hard cardiac events and starting with clinical risk factors, resting wall motion abnormality (RWMA) and inducible WMA offered incremental prognostic information to the model. The addition of either visual SENC or quantitative myocardial strain rate reserve further added prognostic value. **(A)** That was not the case for strain reserve. **(B)** Analysis of subgroups using the Duke Clinical Score showed that the incremental value of SENC mainly derived from patients with intermediate pre-test probability, whereas differences were minor in patients either at low or high risk. Abbreviations as in Figure 1.

Grouping of patients into subgroups using the Duke Clinical Score showed that the incremental value of SENC over conventional WMA mainly derives from its ability to better risk stratify patients with intermediate pre-test probability for CAD. This observation makes the translation of our findings to the clinical realm even more attractive, as patients at intermediate risk for CAD are most appropriate for noninvasive stress testing according to current guidelines (23).

Study limitations. Late gadolinium enhancement is a clinically established technique for the detection of myocardial infarction and was recently shown to predict adverse outcome independent of segmental WMA (24,25) and perfusion defects during stress testing (26). In our study, the presence of delayed enhancement was not systematically analyzed, and is the major limitation of our study. In addition, our study population encompasses a high proportion of patients at high risk, limiting the extrapolation of our findings to ambulatory settings with lower risk cohorts. Moreover, the number of hard cardiac events was relatively small, and although a limited set of parameters was included in multivariable analysis (maximum = 5) a certain amount of over-fitting is still expected with our analysis. Furthermore, the real success rate of DS-MRI was relatively low.

JACC Vol. 58, No. 11, 2011
September 6, 2011:1140–9

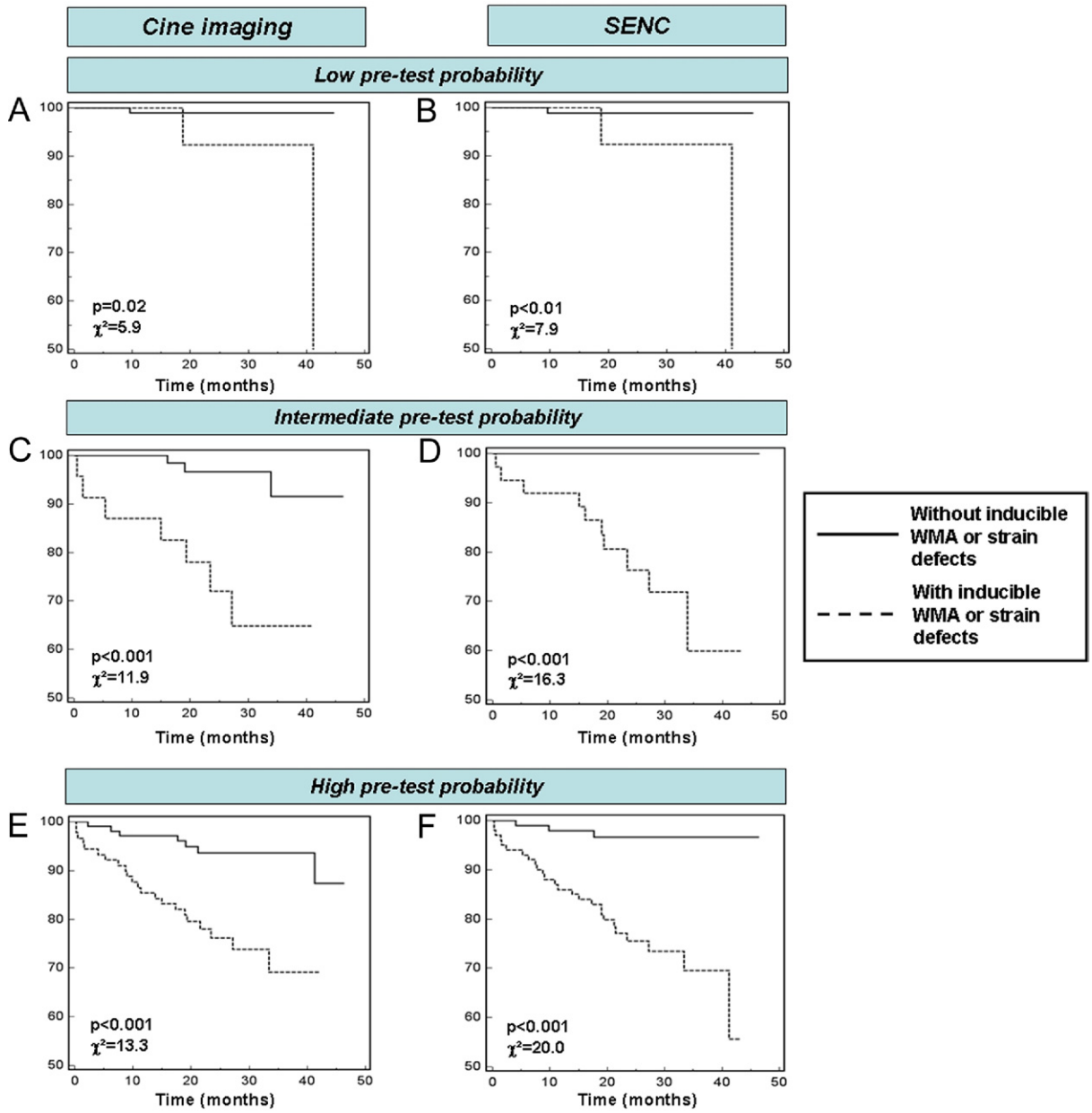

Figure 5 Subgroup Survival Analysis by Pre-Test Probability

SENC allowed for better risk stratification of patients with intermediate pre-test probability. **(C, D)** Patients who had normal strain response within this group exhibited no hard events within the follow-up period, whereas patients who had normal wall motion still experienced a cumulative event rate of >5%. **(A, B, E, F)** Conversely, the predictive value of the 2 techniques was similar in patients with either low or high pre-test probability. **Solid lines** indicate patients without inducible WMA or strain defects; **dashed lines** indicate patients with inducible WMA or strain defects. Abbreviations as in Figure 1.

However, in the absence of claustrophobia and large body habitus, diagnostic stress examinations were obtained in 324 of 361 patients (90%), comparable to the numbers reported in previous MRI (4,27) and echocardiography studies (28). In addition, visual SENC improved sensitivity for CAD detection compared to WMA, while specificity was slightly lower, and a nonsignificant trend for higher accuracy was observed. The slightly lower specificity of SENC for ischemia detection may partially be attributed to induction of myocardial ischemia detectable by SENC: 1) in myocardial regions supplied by mildly stenotic vessels (e.g., 40% to 50%), which were classified as nonischemic by the predefined angiographic criteria (5,6); or 2) in myocardial segments with microvascular impairment in the absence of coronary lumen narrowing (29). Finally, our method comparison may suffer from a methodological mismatch, in that

the assessment of wall motion that corresponds to radial myocardial function was assessed only visually, whereas SENC, which characterizes circumferential and longitudinal shortening, was assessed both visually and quantitatively.

Conclusions

Our study demonstrates that the assessment of myocardial strain response on SENC images aids the accurate identification of patients at high risk for future hard cardiac events and revascularization procedures. The prognostic value of visual SENC and quantitative strain rate reserve are higher than that provided by conventional atherogenic risk factors, resting and inducible WMA by cine imaging. The incremental prognostic value of SENC is mainly attributed to the more accurate risk stratification of patients with intermediate pre-test probability, which represents the main target group for noninvasive diagnostic stress procedures.

Reprint requests and correspondence: Dr. Grigorios Korosoglou, Department of Cardiology, University of Heidelberg, Im Neuenheimer Feld 410, Heidelberg 69120, Germany. E-mail: gkorosoglou@hotmail.com.

REFERENCES

1. Nagel E, Lehmkuhl HB, Bocksch W, et al. Noninvasive diagnosis of ischemia-induced wall motion abnormalities with the use of high-dose dobutamine stress MRI: comparison with dobutamine stress echocardiography. Circulation 1999;99:763–70.
2. Paetsch I, Jahnke C, Wahl A, et al. Comparison of dobutamine stress magnetic resonance, adenosine stress magnetic resonance, and adenosine stress magnetic resonance perfusion. Circulation 2004;110:835–42.
3. Jahnke C, Nagel E, Gebker R, et al. Prognostic value of cardiac magnetic resonance stress tests: adenosine stress perfusion and dobutamine stress wall motion imaging. Circulation 2007;115:1769–76.
4. Korosoglou G, Elhmidi Y, Steen H, et al. Prognostic value of high-dose dobutamine stress magnetic resonance imaging in 1,493 consecutive patients: assessment of myocardial wall motion and perfusion. J Am Coll Cardiol 2010;56:1225–34.
5. Korosoglou G, Lehrke S, Wochele A, et al. Strain-encoded CMR for the detection of inducible ischemia during intermediate stress. J Am Coll Cardiol Img 2010;3:361–71.
6. Korosoglou G, Lossnitzer D, Schellberg D, et al. Strain-encoded cardiac MRI as an adjunct for dobutamine stress testing: incremental value to conventional wall motion analysis. Circ Cardiovasc Imaging 2009;2:132–40.
7. Pryor DB, Shaw L, McCants CB, et al. Value of the history and physical in identifying patients at increased risk for coronary artery disease. Ann Intern Med 1993;118:81–90.
8. Meijboom WB, van Mieghem CA, Mollet NR, et al. 64-slice computed tomography coronary angiography in patients with high, intermediate, or low pre-test probability of significant coronary artery disease. J Am Coll Cardiol 2007;50:1469–75.
9. Frahm J, Hanicke W, Bruhn H, Gyngell ML, Merboldt KD. High-speed STEAM MRI of the human heart. Magn Reson Med 1991;22:133–42.
10. Cerqueira MD, Weissman NJ, Dilsizian V, et al. Standardized myocardial segmentation and nomenclature for tomographic imaging of the heart: a statement for healthcare professionals from the Cardiac Imaging Committee of the Council on Clinical Cardiology of the American Heart Association. Circulation 2002;105:539–42.
11. Cornel JH, Bax JJ, Elhendy A, et al. Biphasic response to dobutamine predicts improvement of global left ventricular function after surgical revascularization in patients with stable coronary artery disease: implications of time course of recovery on diagnostic accuracy. J Am Coll Cardiol 1998;31:1002–10.
12. Kramer MS, Feinstein AR. Clinical biostatistics. LIV. The biostatistics of concordance. Clin Pharmacol Ther 1981;29:111–23.
13. Pencina MJ, D'Agostino RB Sr., D'Agostino RB Jr., Vasan RS. Evaluating the added predictive ability of a new marker: from area under the ROC curve to reclassification and beyond. Stat Med 2008;27:157–72, discussion 207–12.
14. Bjork Ingul C, Rozis E, Slordahl SA, Marwick TH. Incremental value of strain rate imaging to wall motion analysis for prediction of outcome in patients undergoing dobutamine stress echocardiography. Circulation 2007;115:1252–9.
15. Stanton T, Leano R, Marwick TH. Prediction of all-cause mortality from global longitudinal speckle strain: comparison with ejection fraction and wall motion scoring. Circ Cardiovasc Imaging 2009;2:356–64.
16. Sutherland GR, Di Salvo G, Claus P, D'Hooge J, Bijnens B. Strain and strain rate imaging: a new clinical approach to quantifying regional myocardial function. J Am Soc Echocardiogr 2004;17:788–802.
17. Reant P, Labrousse L, Lafitte S, et al. Experimental validation of circumferential, longitudinal, and radial 2-dimensional strain during dobutamine stress echocardiography in ischemic conditions. J Am Coll Cardiol 2008;51:149–57.
18. Chan J, Hanekom L, Wong C, Leano R, Cho GY, Marwick TH. Differentiation of subendocardial and transmural infarction using two-dimensional strain rate imaging to assess short-axis and long-axis myocardial function. J Am Coll Cardiol 2006;48:2026–33.
19. Tanaka H, Oishi Y, Mizuguchi Y, et al. Three-dimensional evaluation of dobutamine-induced changes in regional myocardial deformation in ischemic myocardium using ultrasonic strain measurements: the role of circumferential myocardial shortening. J Am Soc Echocardiogr 2007;20:1294–9.
20. Winter R, Jussila R, Nowak J, Brodin LA. Speckle tracking echocardiography is a sensitive tool for the detection of myocardial ischemia: a pilot study from the catheterization laboratory during percutaneous coronary intervention. J Am Soc Echocardiogr 2007;20:974–81.
21. Weidemann F, Jung P, Hoyer C, et al. Assessment of the contractile reserve in patients with intermediate coronary lesions: a strain rate imaging study validated by invasive myocardial fractional flow reserve. Eur Heart J 2007;28:1425–32.
22. Weidemann F, Jamal F, Sutherland GR, et al. Myocardial function defined by strain rate and strain during alterations in inotropic states and heart rate. Am J Physiol Heart Circ Physiol 2002;283:H792–9.
23. Heller GV, Stowers SA, Hendel RC, et al. Clinical value of acute rest technetium-99m tetrofosmin tomographic myocardial perfusion imaging in patients with acute chest pain and nondiagnostic electrocardiograms. J Am Coll Cardiol 1998;31:1011–7.
24. Kelle S, Roes SD, Klein C, et al. Prognostic value of myocardial infarct size and contractile reserve using magnetic resonance imaging. J Am Coll Cardiol 2009;54:1770–7.
25. Kwong RY, Chan AK, Brown KA, et al. Impact of unrecognized myocardial scar detected by cardiac magnetic resonance imaging on event-free survival in patients presenting with signs or symptoms of coronary artery disease. Circulation 2006;113:2733–43.
26. Steel K, Broderick R, Gandla V, et al. Complementary prognostic values of stress myocardial perfusion and late gadolinium enhancement imaging by cardiac magnetic resonance in patients with known or suspected coronary artery disease. Circulation 2009;120:1390–400.
27. Wahl A, Paetsch I, Gollesch A, et al. Safety and feasibility of high-dose dobutamine-atropine stress cardiovascular magnetic resonance for diagnosis of myocardial ischaemia: experience in 1000 consecutive cases. Eur Heart J 2004;25:1230–6.
28. Geleijnse ML, Fioretti PM, Roelandt JR. Methodology, feasibility, safety and diagnostic accuracy of dobutamine stress echocardiography. J Am Coll Cardiol 1997;30:595–606.
29. Pilz G, Klos M, Ali E, Hoefling B, Scheck R, Bernhardt P. Angiographic correlations of patients with small vessel disease diagnosed by adenosine-stress cardiac magnetic resonance imaging. J Cardiovasc Magn Reson 2008;10:8.

Key Words coronary artery disease ■ high-dose dobutamine stress testing ■ myocardial strain rate reserve ■ outcome ■ strain-encoded magnetic resonance imaging.

APPENDIX

For supplementary figures, please see the online version of this article.